

Accounts

Dioxygen Activation by Copper Complexes. Mechanistic Insights into Copper Monooxygenases and Copper Oxidases

Shinobu Itoh* and Shunichi Fukuzumi†

Department of Chemistry, Graduate School of Science, Osaka City University,
3-3-138 Sugimoto, Sumiyoshi-ku, Osaka 558-8585

†Department of Material and Life Science, Graduate School of Engineering, Osaka University,
CREST, Japan Science and Technology Corporation, 2-1 Yamada-oka, Suita, Osaka 565-0871

(Received January 21, 2002)

Reactions of copper(I) complexes with molecular oxygen have been examined using a series of *N*-alkyl-bis[2-(2-pyridyl)ethyl]amine tridentate ligands ($^R\text{Py}_2^R$) and *N,N*-dialkyl-2-(2-pyridyl)ethylamine didentate ligands ($^R\text{Py}_1^{R1,R2}$) at low temperature. The tridentate ligands predominantly provide $(\mu\text{-}\eta^2\text{:}\eta^2\text{-peroxo})\text{dicopper(II)}$ complexes (side-on type peroxo complex), while the didentate ligands enhance O–O bond homolysis of the peroxo species to produce bis($\mu\text{-oxo}$)dicopper(III) complexes. With the $(\mu\text{-}\eta^2\text{:}\eta^2\text{-peroxo})\text{dicopper(II)}$ complexes supported by the tridentate ligand, efficient oxygenation of phenolates to the corresponding catechols has been accomplished to provide a good model reaction of tyrosinase. The bis($\mu\text{-oxo}$)dicopper(III) complexes, on the other hand, undergo aliphatic ligand hydroxylation as well as oxygen atom transfer to sulfides to give the corresponding sulfoxides. In the reaction of bis($\mu\text{-oxo}$)dicopper(III) complex with 10-methyl-9,10-dihydroacridine (AcrH_2) and 1,4-cyclohexadiene (CHD), a new active oxygen intermediate such as a $(\mu\text{-oxo})(\mu\text{-oxyl radical})\text{dicopper(III)}$ or a tetranuclear copper-oxygen complex has been suggested to be involved as the real active oxygen species for the C–H bond activation of the external substrates. A mixed valence bis($\mu_3\text{-oxo}$) trinuclear copper(II,II,III) complex has also been assessed using the didentate ligand with the smallest *N*-alkyl substituent (methyl). Mechanistic details of the above reactions as well as ligand effects on the copper(I)-dioxygen reactivity are discussed systematically.

Dioxygen binding and activation are accomplished at several transition-metal sites in biological systems. Clarification of the mechanism and application of such processes have long been one of the most important and attractive research objectives not only in bioinorganic chemistry but also in a numerous and diverse array of catalytic oxidation reactions.^{1,2,3,4,5} Since the crystal structure of oxy-myoglobin was solved in 1980,⁶ a great deal of attention has been paid to the iron-porphyrin systems (so-called *heme proteins*).^{1–5,7} The porphyrin ligands are relatively rigid macrocycles exhibiting very characteristic absorption bands in the visible region. This feature of the porphyrin ligand provides a convenient means to monitor the reactions by UV-vis spectra, enabling us to obtain valuable information about key intermediates of the dioxygen processing fairly easily. A huge number of model compounds (porphyrin derivatives) have also been developed to help our understanding of the chemistry of heme proteins. Thus, the research about (reversible) binding and activation of molecular oxygen by heme proteins has now arrived at a mature stage to unravel very sophisticated functions of the heme proteins.

During the past two decades, a number of metalloproteins

carrying one or more *non-heme* transition-metal center(s) have also been identified as dioxygen-carrier and -activating enzymes (so-called *non-heme proteins*).^{8,9} The majority of these proteins (enzymes) consist of mononuclear or dinuclear iron or copper active sites supported by imidazole and/or carboxylate groups from the peptide backbones. Thus, there could exist a wide variety of active site structures in the non-heme metalloproteins. However, the lack of a common chromophore such as a porphyrin ligand causes featureless spectra of the proteins, making it difficult to study mechanisms of the enzymatic reactions in detail. From these points of view, development of proper model complexes exhibiting spectroscopic characteristics and reactivity similar to those of the non-heme proteins is a challenging endeavor. Success will help not only to uncover the enzymatic functions but also to invent efficient catalysts applicable to catalytic oxygenation reactions. Although model studies of the non-heme proteins are still at a rudimentary stage, recent works have provided significantly important insights into dioxygen binding and activation mechanism by several transition-metal complexes.

In this account, we would like to summarize our recent stud-

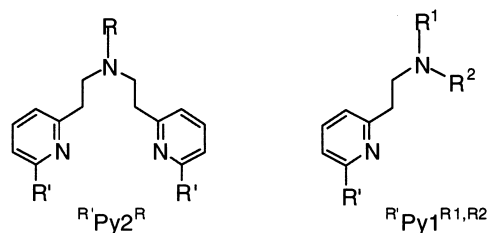


Chart 1.

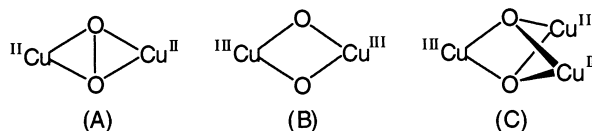


Fig. 1. Structures of (A) (μ - η^2 : η^2 -peroxo)dicopper(II), (B) bis(μ -oxo)dicopper(III), and (C) mixed valence bis(μ_3 -oxo) trinuclear copper(II,II,III) complexes. Ligands are omitted for clarity.

ies on dioxygen activation mechanism by copper complexes, aimed at understanding of the copper(I)-dioxygen reactivity in copper monooxygenases and copper oxidases. In our studies, we have frequently employed a series of 2-(2-pyridyl)ethylamine derivatives as the supporting ligands (Chart 1). Dinucleating ligands carrying bis[2-(2-pyridyl)ethyl]amine tridentate metal binding units were first reported by Karlin and co-workers in the early 1980's, opening a new field of bioinorganic model chemistry of copper proteins (Charts 2 and 4).¹⁰ Their great success together with our recent development in copper/dioxygen chemistry using a series of bis[2-(2-pyridyl)ethyl]amine tridentate ligands (R^1Py2R : two pyridine nitrogens plus one tertiary amine nitrogen) have provided profound insights into the formation and reactivity of the side-on (μ - η^2 : η^2) peroxo dicopper(II) complexes [Fig. 1(A)].¹¹ In addition, we have recently developed a series of 2-(2-pyridyl)ethylamine didentate ligands ($R^1Py1R^{1,R2}$: one pyridine nitrogen plus one tertiary amine nitrogen) that allowed us to assess the chemistry of bis(μ -oxo)dicopper(III) complexes as well as a mixed valence bis(μ_3 -oxo) trinuclear copper(II,II,III) complex [Fig. 1(B) and 1(C)]. We hope the readers will find that significantly rich chemistry does exist in such very simple didentate and tridentate ligand systems.

Formation of (μ - η^2 : η^2 -Peroxo)dicopper(II) Complexes of Tridentate Ligands R^1Py2R

Hemocyanin (Hc), tyrosinase (Tyr) and catechol oxidase (CO) constitute a family of dinuclear copper proteins; these play important roles in dioxygen processing (Hc for reversible O_2 -binding, Tyr and CO for O_2 -activation).¹² Figure 2 shows the active site structure of deoxy form of Hc from *P. interruptus*, where three histidine imidazole residues hold each copper(I) ion.¹³ Both copper ions have distorted trigonal pyramidal structures and are separated by 3.5–3.6 Å from each other.¹⁴ Reaction of deoxy Hc with O_2 affords oxy-hemocyanin (oxy-Hc), the structure of which has also been solved as shown in Fig. 3.¹⁵ Molecular oxygen is bound to the dinuclear copper site to give a side-on (μ - η^2 : η^2) peroxo complex (O–O: 1.4 Å)

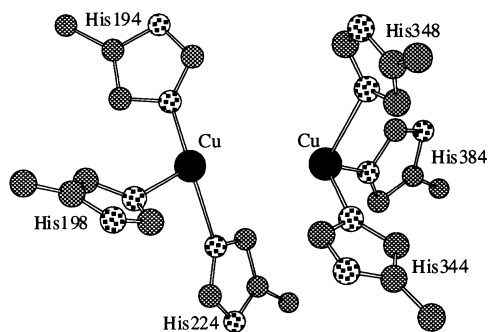


Fig. 2. Active site structure of *P. interruptus* hemocyanin.¹³

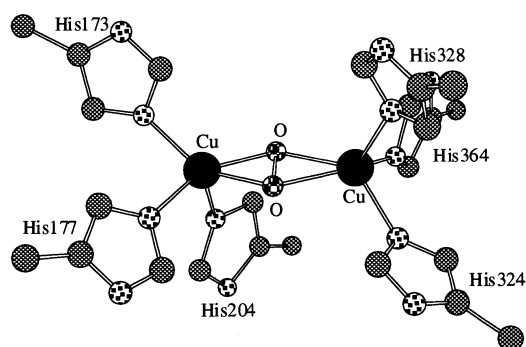


Fig. 3. Active site structure of *L. polyphemus* oxyhemocyanin.¹⁵

which exhibits a strong absorption band at ~ 350 nm ($\epsilon \sim 20,000$ M⁻¹ cm⁻¹) together with a reasonably intense band at ~ 600 nm ($\epsilon \sim 1,000$ M⁻¹ cm⁻¹). These absorption bands have been assigned to $O_2 \rightarrow Cu^{II}$ charge transfer transitions.¹⁶ The side-on peroxo dicopper(II) complex affords an unusually low O–O stretching frequency at ~ 750 cm⁻¹ in the resonance Raman spectrum. Furthermore, this species is ESR silent due to the strong antiferromagnetic interaction between the two copper(II) ions through the peroxo bridge.¹⁶

It should be noted that the side-on peroxo complex was prepared and structurally characterized in a model system several years before the structural determination of oxy-Hc. In Fig. 4 is shown the (μ - η^2 : η^2 -peroxo)dicopper(II) complex of hydrotris(3,5-diisopropyl-1-pyrazolyl)borate ligand.¹⁷

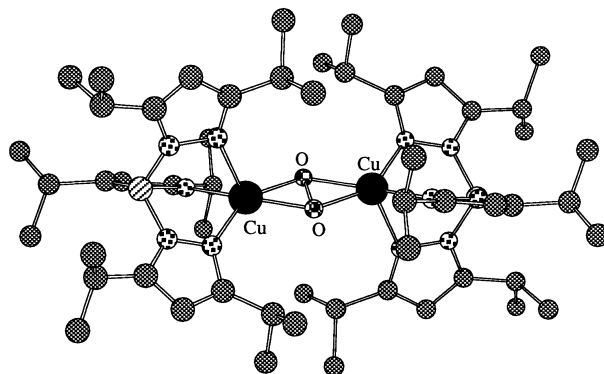


Fig. 4. Chem 3D view of the (μ - η^2 : η^2 -peroxo)dicopper(II) complex of hydrotris(3,5-diisopropyl-1-pyrazolyl)borate ligand.¹⁷

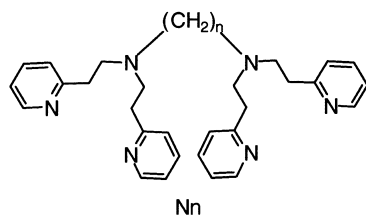


Chart 2.

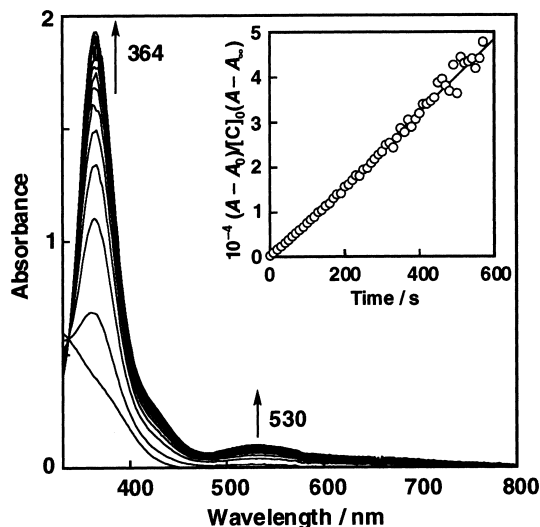
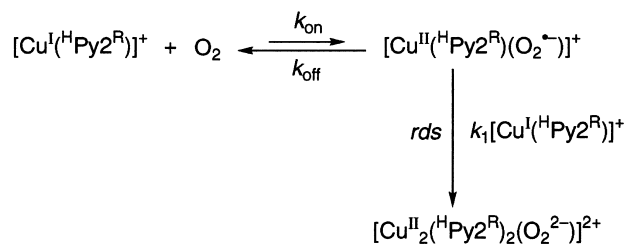


Fig. 5. Spectral change observed upon introduction of O_2 gas into an acetone solution of $[Cu^I(^H\text{Py}2^{Bz-d_2})]PF_6$ (1.5×10^{-4} M) at -94°C . Inset: Second-order plot based on the absorption change at 364 nm.

ris(3,5-diisopropyl-1-pyrazolyl)borate ligand reported by Kitajima, Fujisawa and Moro-oka in 1989.¹⁷ The complex reproduced most of the spectroscopic features of oxy-Hc [UV-vis: $\lambda_{\text{max}} = 349$ nm ($\epsilon = 21,000$ M $^{-1}$ cm $^{-1}$), 551 nm (800 M $^{-1}$ cm $^{-1}$); Raman: 741 cm $^{-1}$ ($^{16}\text{O}-^{16}\text{O}$), 698 cm $^{-1}$ ($^{18}\text{O}-^{18}\text{O}$); ESR silent]. These spectroscopic features strongly indicated the existence of such a binding mode of peroxo ligand in the enzymatic system. This was confirmed by the crystal structure of oxy-Hc five years later, as mentioned above (Fig. 2). The correct prediction of the presence of $\mu\text{-}\eta^2\text{:}\eta^2\text{-peroxo}$ binding mode in oxy-hemocyanin is one of the greatest successes of bioinorganic model chemistry. Reversible dioxygen binding at dinuclear copper(I) sites (functional models of Hc) has also been accomplished in model systems by using poly-pyridine derivatives such as Nn (Chart 2) as the supporting ligand.^{18,19}

The tridentate ligand $^H\text{Py}2^R$ ($R' = \text{H}$ in Chart 1) can also support the $(\mu\text{-}\eta^2\text{:}\eta^2\text{-peroxo})\text{dicopper(II)}$ complex (A). Namely, the copper(I) complexes of $^H\text{Py}2^R$ reacts with molecular oxygen at a low temperature to give a $(\mu\text{-}\eta^2\text{:}\eta^2\text{-peroxo})\text{dicopper(II)}$ complex which exhibits nearly the same spectroscopic characteristics as those of oxy-Hc as well as other reported side-on peroxo model complexes.^{20,21,22,23} Figure 5 shows a typical example of the spectral change for the oxygenation reaction of $[Cu^I(^H\text{Py}2^{Bz-d_2})]PF_6$ ($Bz\text{-}d_2 = \text{-CD}_2\text{Ph}$) at -94°C in acetone, where a strong absorption band at 364 nm ($\epsilon = 26,400$ M $^{-1}$ cm $^{-1}$) together with a small one at 530 nm (1,500



Scheme 1.

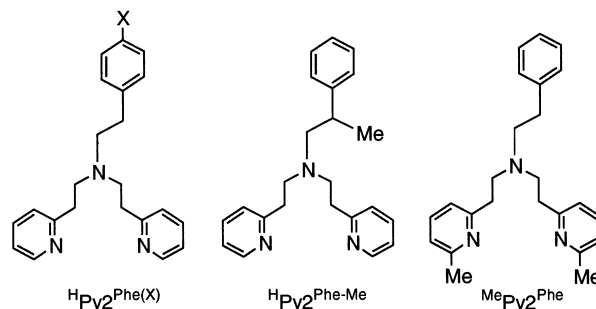


Chart 3.

M $^{-1}$ cm $^{-1}$) gradually develop.²¹ The stoichiometry of Cu: $O_2 = 2:1$ together with a resonance Raman band at 737 cm $^{-1}$ that shifted to 697 cm $^{-1}$ upon ^{18}O -substitution and ESR silence of the oxygenated intermediate unambiguously supported the quantitative formation of the $(\mu\text{-}\eta^2\text{:}\eta^2\text{-peroxo})\text{dicopper(II)}$ complex.^{20,21,24}

The time course for the formation of $(\mu\text{-}\eta^2\text{:}\eta^2\text{-peroxo})\text{dicopper(II)}$ complex obeys second-order kinetics, as shown in the inset of Fig. 5, suggesting that the bimolecular reaction between the monomeric superoxo copper(II) complex $[Cu^{II}(^H\text{Py}2^R)(O_2^{\bullet-})]^+$ and another Cu^I complex is rate determining and that the primary reaction between the Cu^I complex and O_2 is in a rapid equilibrium, where the superoxo species is a minor component (Scheme 1).²² Similar second-order kinetics was observed in the oxygenation reactions of other Cu^I complexes with a series of $^H\text{Py}2^R$ ligands, although the overall rate for the oxygenation reactions varied significantly depending on the type of *N*-alkyl substituent (*R*).²²

One of the most extreme examples was found in the ligand system of $^H\text{Py}2^{\text{Phe-Me}}$ (Phe-Me = $-\text{CH}_2\text{CH}(\text{Me})\text{Ph}$, Chart 3), with which reactivity of the copper(I) complex toward O_2 was almost lost.²⁵ This is a sharp contrast to the fact that the copper(I) complex of $^H\text{Py}2^{\text{Phe(H)}}$ (Phe(H) = $-\text{CH}_2\text{CH}_2\text{Ph}$, Chart 3) readily reacts with O_2 to give the $(\mu\text{-}\eta^2\text{:}\eta^2\text{-peroxo})\text{dicopper(II)}$ complex as in the case of $^H\text{Py}2^{Bz}$ described above.²² Crystal structure study of the copper(I) complex of $^H\text{Py}2^{\text{Phe-Me}}$ has clearly shown that there is a $Cu^I\text{-}\pi$ interaction between the copper(I) ion and the phenyl group of the ligand sidearm, as shown in Fig. 6.²⁵ Existence of such a copper(I)-arene interaction in the copper(I) complex of $^H\text{Py}2^{\text{Phe(H)}}$ ($X = \text{H}$, Chart 3) in non-coordinative organic solvents has also been indicated by the $^1\text{H-NMR}$ analysis and by a characteristic absorption band around 290 nm due to the $Cu^I\text{-}\pi$ interaction.^{25,26,27} The methyl group at the benzylic position of $^H\text{Py}2^{\text{Phe-Me}}$ reduces the degree of freedom of sidearm rotation to make the originally weak

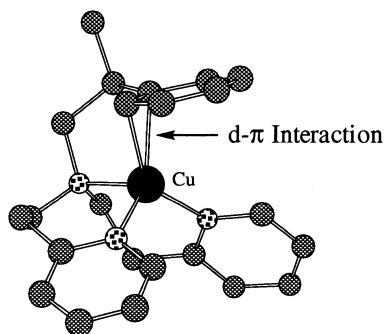
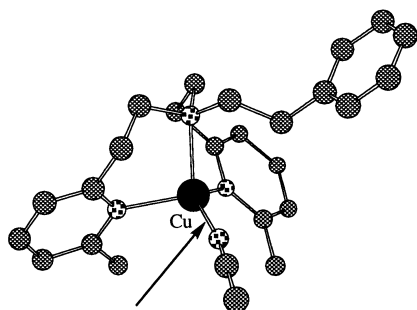


Fig. 6. Chem 3D view of the crystal structure of $[\text{Cu}^{\text{I}}(\text{Py}2^{\text{Phe-Me}})]\text{ClO}_4$. The counter anions and hydrogen atoms are omitted for clarity.²⁵

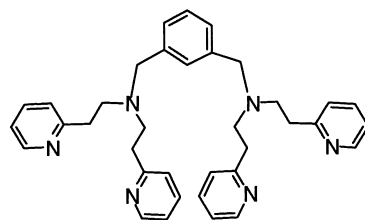


Stronger binding of CH_3CN

Fig. 7. Chem 3D view of the crystal structure of $[\text{Cu}^{\text{I}}(\text{MePy}2^{\text{Phe}})(\text{CH}_3\text{CN})]\text{ClO}_4$. The counter anions and hydrogen atoms are omitted for clarity.²⁵

$\text{Cu}^{\text{I}}-\pi$ interaction stronger in $[\text{Cu}^{\text{I}}(\text{HPy}2^{\text{Phe-Me}})]^+$, thus inhibiting the reaction with O_2 (k_{on} process in Scheme 1). The dioxygen-reactivity of the copper(I) complexes with a series of $\text{HPy}2^{\text{Phe(X)}}$ can be finely tuned (an order of magnitude) by changing the strength of the $\text{Cu}^{\text{I}}-\pi$ interaction with different p -substituents ($\text{X} = \text{OMe}, \text{Me}, \text{H}, \text{Cl}, \text{NO}_2$).²⁸

Introduction of methyl group into the 6-position of the pyridine nuclei to make $\text{MePy}2^{\text{Phe}}$ (Chart 3) resulted in observation of another interesting feature in the copper(I)-dioxygen reactivity.²⁵ Namely, ligand $\text{MePy}2^{\text{Phe}}$ gave a copper(I) complex with a distorted tetrahedral geometry, which consists of three nitrogen atoms of the ligand and one nitrogen atom of the bound CH_3CN (Fig. 7).²⁵ Steric repulsion between the 6-methyl group on the pyridine nucleus of $\text{MePy}2^{\text{Phe}}$ and the metal ion of the complex prevents the copper(I) complex from adaptation to a three-coordinate geometry which must have a shorter $\text{Cu}-\text{N}(\text{pyridine})$ distance ($\sim 1.88 \text{ \AA}$). Thus, the four-coordinate copper(I) complex $[\text{Cu}^{\text{I}}(\text{MePy}2^{\text{Phe}})(\text{CH}_3\text{CN})]^+$ with a longer $\text{Cu}-\text{N}$ bond ($1.98\text{--}2.13 \text{ \AA}$) becomes favorable, resulting in rather strong binding of CH_3CN to the metal ion. The strong binding of CH_3CN also inhibits the access of O_2 to the metal center, making the copper(I) complex of $\text{MePy}2^{\text{Phe}}$ less reactive toward dioxygen as in the case of ligand $\text{HPy}2^{\text{Phe-Me}}$.²⁵ Thus, even the small perturbation induced by the methyl substitution at the benzylic position of the ligand sidearm in $\text{HPy}2^{\text{Phe-Me}}$ and at the 6-position of pyridine nucleus in $\text{MePy}2^{\text{Phe}}$ led to a drastic change in the structure and reactivity of the copper(I) complexes.



XYL
Chart 4.

Oxygenation of Phenolates to Catechols by the $(\mu-\eta^2:\eta^2\text{-Peroxo})\text{dicopper(II)}$ Complex (Model Reaction of Tyrosinase)

Tyrosinase (Tyr) catalyzes oxygenation of phenols to catechols (phenolase activity) and the subsequent two-electron oxidation of catechols to the corresponding *o*-quinones (catecholase activity).¹² Catechol oxidase (CO) exhibits only the catecholase activity.¹² Chemical and spectroscopic studies have indicated that Tyr and CO have a similar dinuclear copper active site, nearly identical to that found in hemocyanin, where a $(\mu-\eta^2:\eta^2\text{-peroxo})\text{dicopper(II)}$ species is also generated by the reaction of the reduced dicopper(I) form and O_2 .^{8,12,29} Karlin and coworkers reported an *aromatic ligand hydroxylation* by O_2 using a dinuclear copper(I) complex supported by ligand XYL (Chart 4).^{30,31} The mechanistic studies have indicated that the aromatic ligand hydroxylation reaction involves an *electrophilic attack* on the arene ring by a $(\mu-\eta^2:\eta^2\text{-peroxo})\text{dicopper(II)}$ intermediate.^{32,33,34} After their finding, several examples of the aromatic ligand hydroxylation have also been reported using a similar type of *m*-xylyl dinucleating ligands.^{35,36} With respect to the intermolecular reactions between phenols and the peroxo intermediate, however, most of the reactions so far reported afford a C–C coupling dimer as a major product.^{37,38,39,40,41,42} Thus, such reactions do not provide valuable mechanistic insights into the catechol formation via intermolecular reactions between the peroxo intermediate and phenol derivatives.

We have recently found that efficient conversion of phenol derivatives to the corresponding catechols can be achieved by the intermolecular reactions of the $(\mu-\eta^2:\eta^2\text{-peroxo})\text{dicopper(II)}$ complex supported by the tridentate ligand $\text{HPy}2^{\text{Bz-d2}}$ with lithium salts of phenols.²¹ Namely, the reactions of lithium salts of *p*-substituted phenols ($p\text{-X-C}_6\text{H}_4\text{OLi}$; $\text{X} = t\text{-Bu}, \text{Me}, \text{Cl}, \text{Br}$ and CO_2Me) and the peroxo complex resulted in formation of the corresponding catechols in good yields ($> 99, 69, 90, 79$ and 60% , respectively, based on the peroxo complex), but none of the corresponding *o*-quinone derivatives, the C–C and C–O coupling dimers, was obtained from the final reaction mixture.²¹ Thus, the catechols were formed as a solely isolable product nearly quantitatively by intermolecular reactions between the peroxo complex and the phenolates. Isotope labeling experiment using $^{18}\text{O}_2$ confirmed that the origin of one of the two oxygen atoms of the catechol product was molecular oxygen.²¹ In contrast to such an efficient catechol formation by the peroxo complex, no catechol was formed when a bis(μ -oxo)dicopper(III) complex generated by using didentate ligand $\text{HPy}1^{\text{Et,Bz-d2}}$ (vide infra) was employed under otherwise

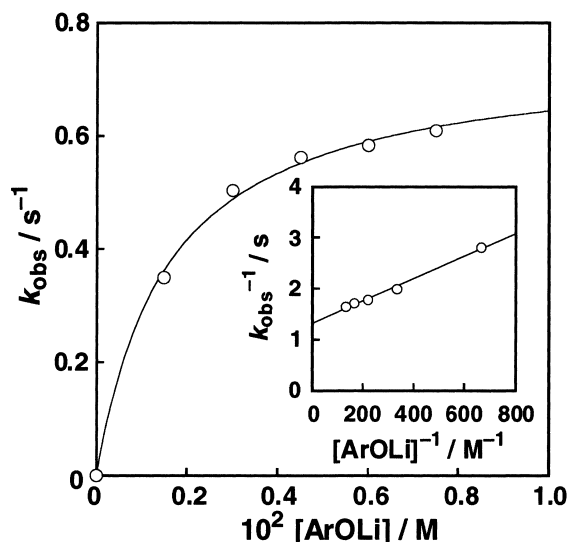


Fig. 8. Plot of k_{obs} against the substrate concentration for the reaction of $[\text{Cu}^{\text{II}}_2(\text{H}^{\text{t}}\text{Py}2^{\text{Bz-d2}})_2(\mu\text{-O}_2)]^{2+}$ (7.5×10^{-5} M) in acetone at -94°C with lithium 4-chlorophenolate. Inset: plot of k_{obs}^{-1} vs $[p\text{-Cl-C}_6\text{H}_4\text{OLi}]^{-1}$.²¹

Table 1. Formation Constants (K_f) and Rate Constants (k_{ox}) for the Reaction between $[\text{Cu}^{\text{II}}_2(\text{H}^{\text{t}}\text{Py}2^{\text{Bz-d2}})_2(\mu\text{-O}_2)](\text{PF}_6)_2$ and $p\text{-X-C}_6\text{H}_4\text{OLi}$ in Acetone at -94°C ^{a)}

X	K_f/M^{-1}	$k_{\text{ox}}/\text{s}^{-1}$
<i>t</i> -Bu	— ^{b)}	— ^{b)}
Me	— ^{b)}	— ^{b)}
Br	465	0.93
Cl	570	0.76
F	948	0.63
COMe	493	0.086
COOMe	940	0.083

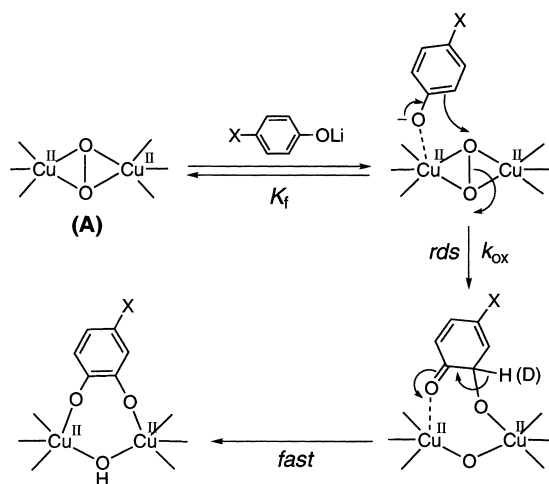
a) Kinetic studies on the oxidation of phenolates with more strongly electron-withdrawing substituents such as $-\text{CN}$ and $-\text{NO}_2$ could not be carried out accurately because of the strong absorption bands due to the phenolate substrates themselves in the visible region.

b) Too fast to be determined.

the same experimental conditions.²¹

The reactions were followed by low-temperature UV-vis spectra. The reaction rates obeyed pseudo-first-order kinetics, and plot of the pseudo-first-order rate constant k_{obs} against the substrate concentration afforded a Michaelis–Menten type saturation curve, as shown in Fig. 8.²¹ This indicates complex formation between the substrate and the peroxo intermediate in the course of the reaction. Such a complex formation prior to the oxygenation, together with the absence of the C–C coupling product, rules out an electron transfer pathway from the substrate to the peroxo intermediate to produce a free radical species.⁴³ From the double reciprocal plot according to the equation, $1/k_{\text{obs}} = 1/k_{\text{ox}} + (1/K_f k_{\text{ox}})(1/[\text{ArOLi}])$ (Lineweaver–Burk type plot, inset of Fig. 8), was obtained the formation constant K_f and the rate constant k_{ox} for the oxidation process, listed in Table 1.

The observed rate constants for *p*-*tert*-butyl and *p*-methyl



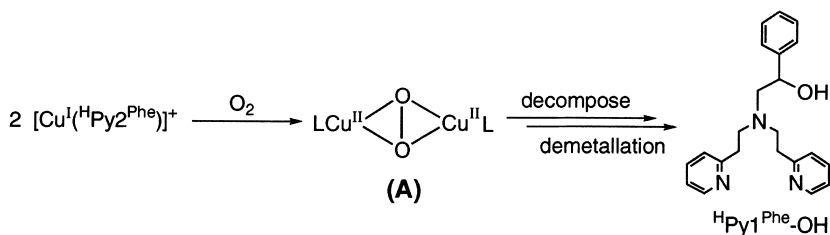
Scheme 2.

phenolate ($X = t\text{-Bu}$ and Me) were, however, too fast to be determined accurately. Thus, the reactivity of the substrate increases drastically with increasing the electron-donating ability of the *p*-substituent, whereas the K_f values are rather insensitive to the electronic effects of the *p*-substituents. In addition, no kinetic deuterium isotope effect was observed as in the case of the enzymatic reaction, when $p\text{-Cl-C}_6\text{D}_4\text{OLi}$ was used as the substrate instead of $p\text{-Cl-C}_6\text{H}_4\text{OLi}$ ($k_{\text{ox}}^{\text{H}}/k_{\text{ox}}^{\text{D}} = 1 \pm 0.1$).²¹

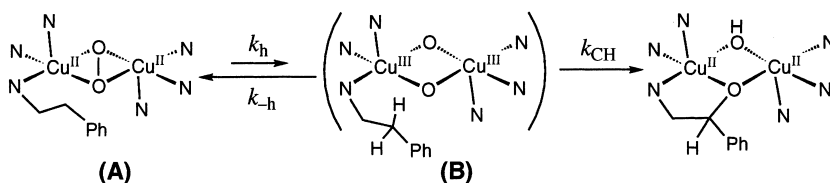
In the enzymatic mechanism of Tyr, there is ongoing controversy with respect to the timing of the O–O bond cleavage of the peroxo intermediate: (i) before, (ii) simultaneous with, or (iii) after the C–O bond formation.^{12,44} In the case of (i), bis($\mu\text{-oxo}$)dicopper(III) complex might be an active oxygen species. In our model system, however, no catechol formation was detected in the reaction with the bis($\mu\text{-oxo}$) complex of $\text{H}^{\text{t}}\text{PyI}^{\text{EtBz-d2}}$.²¹ On the other hand, if the O–O bond cleavage occurred after the C–O bond formation (case iii), an (alkylperoxo)copper(II) type intermediate ($\text{R-O-O-Cu}^{\text{II}}$) would be involved. Such a reactive species has been shown to decompose leading to direct formation of a quinone product.⁴⁵ In our system, however, only traces of the corresponding quinone products were obtained.²¹ Thus, all our results are consistent with the mechanism of case (ii). Namely, the oxygenation of exogenous phenolates to the corresponding catechols by the ($\mu\text{-}\eta^2\text{:}\eta^2\text{-peroxo}$)dicopper(II) complex (A) proceeds via an *electrophilic aromatic substitution mechanism*, where the oxygenation of the substrate (C–O bond formation) occurs simultaneously with the O–O bond cleavage of the peroxo intermediate (Scheme 2). Furthermore, it is obvious that deprotonation of the substrate prior to the reaction is essential, since only the C–C coupling dimer was obtained when the phenol itself was used instead of the phenolate as the exogenous substrate.⁴³ This suggests that deprotonation of the phenol substrates may also occur in the substrate-binding process of the enzymatic system.

Aliphatic Ligand Hydroxylation by Cu_2/O_2 Species

The ligands with a phenethyl substituent ($\text{R} = \text{Phe}$) brought about another interesting aspect of the copper(I)-dioxygen reactivity. The copper(I) complex supported by $\text{H}^{\text{t}}\text{Py}2^{\text{Phe}}$ similar-



Scheme 3.



Scheme 4.

ly reacted with O_2 in a 2:1 ratio at -80°C to give a $(\mu-\eta^2:\eta^2\text{-peroxo})\text{dicopper(II)}$ intermediate. The peroxo complex (A) exhibited a characteristic absorption band at 362 nm together with a small one at 526 nm and a resonance Raman band at 746 cm^{-1} that shifted to 704 cm^{-1} upon $^{18}\text{O}_2$ substitution.²² At a prolonged reaction time, this intermediate gradually decomposed, leading to a *quantitative aliphatic ligand hydroxylation* at its benzylic position of the *N*-alkyl substituent (Phe) (Scheme 3).^{22,46} The mass spectrum of the modified ligand obtained in the reaction using $^{18}\text{O}_2$ confirmed that the origin of the oxygen atom of the OH group was molecular oxygen.²² Since much of the interest at that time had been focused on the Karlin's *aromatic ligand hydroxylation* reactions in the dinuclear copper complex supported by XYL, our finding of the *quantitative aliphatic ligand hydroxylation* reaction using the simple tridentate ligand⁴⁶ was a great surprise to researchers in this field.

Kinetic deuterium isotope effect on the ligand hydroxylation process was examined using HPy2^{Phe} and $\text{HPy2}^{\text{Phe-d}_4}$ (Phe = $-\text{CH}_2\text{CH}_2\text{Ph}$ and $\text{Phe-d}_4 = -\text{CD}_2\text{CD}_2\text{Ph}$) at various temperatures; the activation parameters were determined as $\Delta H_{\text{H}}^\ddagger = 6.7 \pm 0.2\text{ kcal mol}^{-1}$, $\Delta S_{\text{H}}^\ddagger = -37.0 \pm 0.7\text{ cal K}^{-1}\text{ mol}^{-1}$, $\Delta H_{\text{D}}^\ddagger = 9.6 \pm 0.2\text{ kcal mol}^{-1}$, $\Delta S_{\text{D}}^\ddagger = -25.6 \pm 0.7\text{ cal K}^{-1}\text{ mol}^{-1}$ by the Eyring plots shown in Fig. 9 (line H vs line D).²² The kinetic isotope effect (KIE) for the ligand hydroxylation process was 5.9 at -80°C in THF, but the KIE value decreases to 1.8 at -40°C .²² These KIE values are significantly smaller than those observed in the oxidative *N*-dealkylation reaction (C-H bond cleavage) in the bis(μ -oxo)dicopper(III) core supported by *i*-Pr₃-TACN ($k_{\text{H}}/k_{\text{D}} = 26$) and Bz₃-TACN ($k_{\text{H}}/k_{\text{D}} = 40$) at -40°C in THF (R₃-TACN: 1,4,7-trialkyl-1,4,7-triazacyclononane),⁴⁷ and in the hydrocarbon hydroxylation by a high-valent bis(μ -oxo)diiron(III,IV) complex $[\text{Fe}_2(\mu\text{-O})_2(\text{TPA})_2]^{3+}$ {TPA = tris(2-pyridylmethyl)amine} ($k_{\text{H}}/k_{\text{D}} = 20$ at -40°C).⁴⁸ More interestingly, extrapolation of the Eyring plots gave a KIE value of unity at -16°C as shown in Fig. 9.

Based on the results of the kinetic deuterium isotope effects, we proposed that the $(\mu-\eta^2:\eta^2\text{-peroxo})\text{dicopper(II)}$ species was not a real active oxygen intermediate for the aliphatic C-H

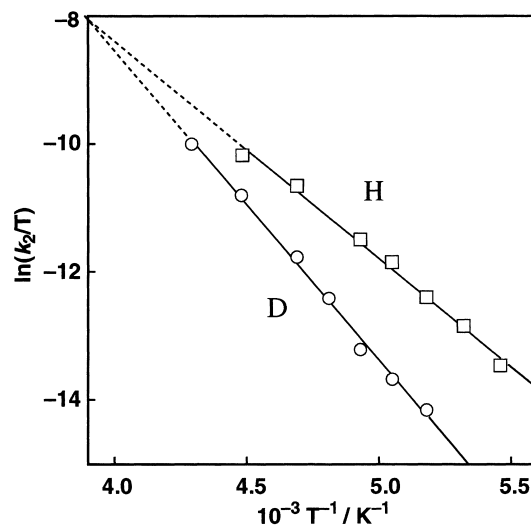


Fig. 9. Eyring plot *S* for the ligand hydroxylation of (H) $[\text{Cu}^{\text{I}}(\text{HPy2}^{\text{Phe}})]\text{PF}_6$ and (D) $[\text{Cu}^{\text{I}}(\text{HPy2}^{\text{Phe-d}_4})]\text{PF}_6$ by O_2 in THF.²²

bond activation. We suggested that O-O bond homolysis of the peroxo intermediate (A) would occur prior to the ligand hydroxylation reaction (Scheme 4).²² If the O-O bond homolysis is the sole rate-determining step in the ligand hydroxylation process, the KIE value would be 1.0. The observed small KIE values in the present system suggest that the O-O bond homolysis (k_{h}) is much slower than the back reaction ($k_{-\text{h}}$) which competes with the facile C-H bond activation (k_{CH}). In such a case, the observed rate constant *k* is given by Eq. 1.

$$k = k_{\text{h}}k_{\text{CH}}/(k_{-\text{h}} + k_{\text{CH}}) \quad (1)$$

The O-O bond homolysis may be largely the rate-determining step, i.e., $k_{\text{CH}} \gg k_{-\text{h}}$, but the ligand perdeuteration may result in a significant decrease in the rate of the C-D cleavage (k_{CD}), which then becomes partially rate-determining. Small *p*-substituent effects (X = Me, H, Cl, NO_2 in $\text{HPy2}^{\text{Phe(X)}}$, see

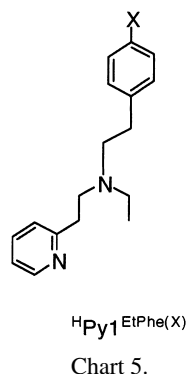


Chart 3) observed on the hydroxylation process are also consistent with the proposed mechanism where the ligand hydroxylation process is not a rate-determining step.²² The observed solvent effects on the ligand hydroxylation process, in which the rate is in the order: THF > acetone > CH₃OH > CH₂Cl₂, are also consistent with the solvent effects in the *i*-Pr₃TACN ligand system,⁴⁹ where the bis(μ -oxo)dicopper(III) complex was predominantly produced in THF while the (μ - η^2 : η^2 -peroxo)dicopper(II) complex was the major component in CH₂Cl₂.²² However, we could not detect the putative bis(μ -oxo)dicopper(III) species (**B**) directly in the tridentate ligand system (Scheme 4).²²

Ligand modification of the tridentate ligand HPy2^{R} by removing one of the pyridine nuclei to make the didentate ligand $\text{HPy1}^{\text{Et,Phe(X)}}$ (X = OMe, Me, H, Cl, NO₂ in Chart 5) brought about a breakthrough, enabling us to detect the bis(μ -oxo)dicopper(III) complex (**B**) directly in the aliphatic ligand hydroxylation reaction.⁵⁰ Namely, the copper(I) complex, $[\text{Cu}^{\text{I}}(\text{HPy1}^{\text{Et,Phe(H)-d4}})(\text{CH}_3\text{CN})]\text{PF}_6$, reacted with O₂ in acetone at -90 °C to afford an oxygenated intermediate exhibiting an ab-

sorption band at 402 nm ($\epsilon = 17,700 \text{ M}^{-1} \text{ cm}^{-1}$) and a resonance Raman band ($\lambda_{\text{ex}} = 457.9 \text{ nm}$) at 607 cm⁻¹ that shifted to 578 cm⁻¹ upon ¹⁸O₂-substitution (Fig. 10).⁵⁰ The stoichiometry was determined as Cu:O₂ = 2:1 by manometry and the resulting compound was ESR-silent.⁵⁰ All these features are very close to those of the reported bis(μ -oxo)dicopper(III) complexes,^{49,51,52,53,54,55} demonstrating that the intermediate generated in the didentate ligand system has a bis(μ -oxo)dicopper(III) core.⁵⁰ As in the case of the tridentate ligand system discussed above, the formation of the bis(μ -oxo)dicopper(III) complex obeyed second-order kinetics with respect to concentration of the starting Cu^I complex. This indicates that the bimolecular reaction between an initially formed monomeric superoxo copper(II) complex, $[\text{Cu}^{\text{II}}(\text{HPy1}^{\text{Et,Phe(H)-d4}})(\text{O}_2^{\bullet-})]^+$, and another Cu^I starting compound is rate-determining and that the resulting (μ -peroxo)dicopper(II) intermediate, $[\text{Cu}^{\text{II}}_2(\text{HPy1}^{\text{Et,Phe(H)-d4}})_2(\mu\text{-O}_2)]^{2+}$, is rapidly converted to the bis(μ -oxo)dicopper(III) species probably through the (μ - η^2 : η^2 -peroxo)dicopper(II) complex.⁵⁰

The bis(μ -oxo)dicopper(III) intermediate supported by $\text{HPy1}^{\text{Et,Phe(H)}}$ gradually decomposed, leading to a quantitative benzylic hydroxylation of the ligand sidearm (phenethyl group). In this case as well, the origin of the oxygen atom of the OH group was confirmed as molecular oxygen by ¹⁸O-labeling experiment.⁵⁰ Kinetic studies of the ligand hydroxylation revealed it to be a first-order process that presumably involves intramolecular decay of the bis(μ -oxo)dicopper(III) intermediate, and a large kinetic deuterium isotope effect (KIE = 35.4 at -80 °C) was obtained.⁵⁰ In addition, Hammett plot of the first-order rate constant against σ^+ gave $\rho = -1.48$ ($\text{HPy1}^{\text{Et,Phe(X)}}$; X = OMe, Me, H, Cl, NO₂).⁵⁰ Overall, the activation parameters ($\Delta H_{\text{H}}^\ddagger = 9.3 \pm 0.1 \text{ kcal mol}^{-1}$, $\Delta S_{\text{H}}^\ddagger = -17.4 \pm 0.5 \text{ cal K}^{-1} \text{ mol}^{-1}$, $\Delta H_{\text{D}}^\ddagger = 12.6 \pm 0.1 \text{ kcal mol}^{-1}$, $\Delta S_{\text{D}}^\ddagger = -7.4 \pm 0.5 \text{ cal K}^{-1} \text{ mol}^{-1}$), KIE, and ρ value for the ligand hydroxylation are similar to those measured previously for the oxidative *N*-dealkylation reaction of the Tolman's bis(μ -oxo)dicopper(III), $[(i\text{-Pr}_3\text{TACN})_2(\text{Cu})_2(\mu\text{-O}_2)](\text{ClO}_4)_2$.⁴⁷ This indicates that a mechanism for the benzylic hydroxylation is similar to that suggested for the *N*-dealkylation reaction, which involves either hydrogen atom abstraction by the bis(μ -oxo)dicopper(III) core followed by hydroxyl rebound or its concerted variant (Scheme 5).⁵⁰

Thus, using the didentate ligand $\text{HPy1}^{\text{Et,Phe(X)}}$, we succeeded in generating the distinct bis(μ -oxo)dicopper(III) complex (**B**), which is shown to be the reactive intermediate for the aliphatic ligand hydroxylation.⁵⁰ As described above, a similar hydroxylation occurred in the system supported by the tridentate ligand $\text{HPy2}^{\text{Phe(X)}}$, but the kinetic data showed that intramolecular isomerization [peroxo \rightarrow bis(μ -oxo)] instead of C-H bond breaking was rate-controlling.²² Thus, a simple change in the denticity of the supporting ligand results in an important shift in the relative rates of O-O and C-H bond scission in these dicopper compounds. These results suggest the possible importance of similar ligand effects on related pathways traversed during aliphatic hydroxylation by copper-containing enzymes such as particulate methane monooxygenase (pMMO) and other synthetic systems.

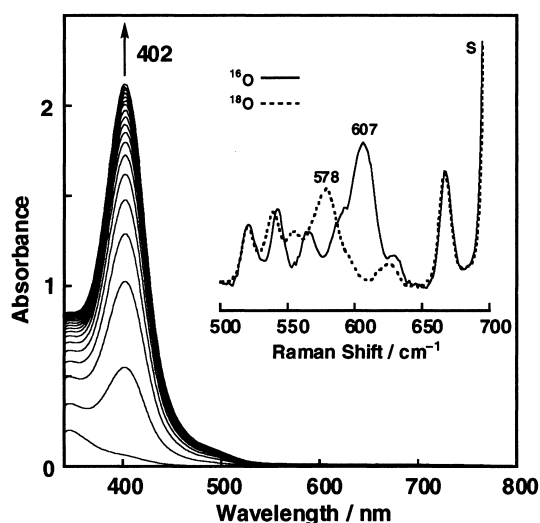
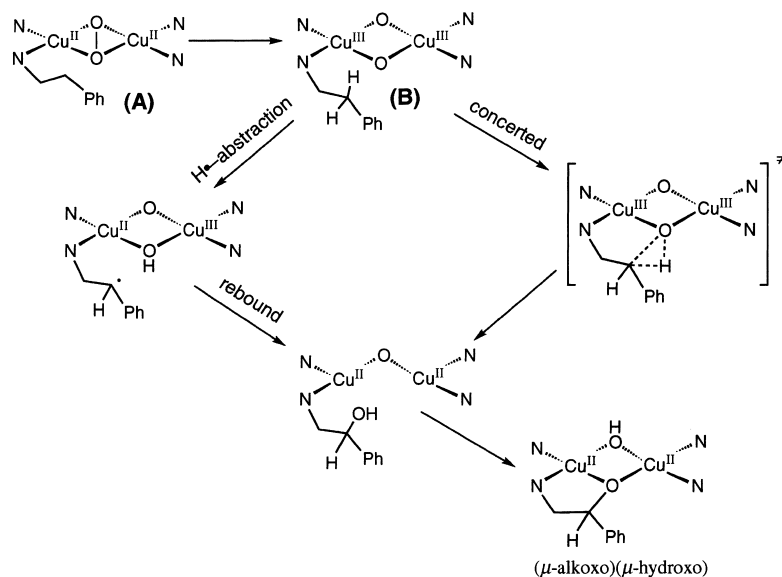
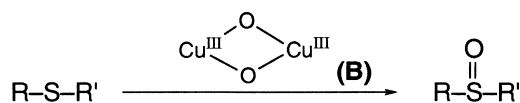


Fig. 10. Spectral change observed upon introduction of O₂ gas into an acetone solution of $[\text{Cu}^{\text{I}}(\text{HPy1}^{\text{Et,Phe(H)-d4}})(\text{CH}_3\text{CN})]\text{PF}_6$ ($2.5 \times 10^{-4} \text{ M}$) at -90 °C. Inset: resonance Raman spectra of frozen solutions of $[\text{Cu}^{\text{III}}_2(\text{HPy1}^{\text{Et,Phe(H)-d4}})_2(\mu\text{-}^{16}\text{O}_2)](\text{PF}_6)_2$ (solid line) and $[\text{Cu}^{\text{III}}_2(\text{HPy1}^{\text{Et,Phe(H)-d4}})_2(\mu\text{-}^{18}\text{O}_2)](\text{PF}_6)_2$ (dashed line) in acetone-*d*₆; s denotes a solvent band.⁵⁰



Scheme 5.



Scheme 6.

Oxo-Transfer Reaction by the Bis(μ-oxo)dicopper(III) Complex

Oxygen atom transfer from metal-oxo species to organic or inorganic substances is ubiquitous not only in a wide variety of biological processes but also in numerous catalytic oxygenation reactions.⁵ Much attention has already been paid to the oxygen transfer reactions catalyzed by iron porphyrin complexes as well as a series of model compounds of non-heme iron oxygenases.^{1-5,7} However, little is known about the oxygen atom transfer reaction of distinct copper-active oxygen species.^{21,22,41,50,56,57} Thus, it is highly desired to investigate the reactivities of dinuclear copper dioxygen complexes toward *intermolecular* oxygen atom transfer reactions not only to uncover the dioxygen activation mechanism by copper monooxygenases but also to develop an efficient catalyst for selective oxidation by dioxygen. In this context, we have recently found the first example of oxygenation of sulfides to the corresponding sulfoxides by the distinct bis(μ-oxo)dicopper(III) complex (B) supported by the didentate ligand ^HPy1^{EtBz-d2} (Scheme 6).⁵⁸

Addition of thioanisole to an acetone solution of the bis(μ-oxo)dicopper(III) complex at $-80\text{ }^{\circ}\text{C}$ under anaerobic conditions resulted in a spectral change that is shown in Fig. 11.⁵⁸ The characteristic absorption band at 400 nm ($\epsilon = 16,500\text{ M}^{-1}\text{ cm}^{-1}$) due to the bis(μ-oxo)dicopper(III) complex (spectrum a) is readily converted to the spectrum (b) ($\lambda_{\text{max}} = 398\text{ nm}$, $\epsilon = 8,620\text{ M}^{-1}\text{ cm}^{-1}$), the intensity of which further decreases slowly, as shown in the inset of Fig. 11. Thus, the present reaction consists of two distinct steps. From the final reaction mixture, the oxygenation product, methyl phenyl sulfoxide, was isolated in 83% yield based on the bis(μ-oxo) complex.⁵⁸ Iso-

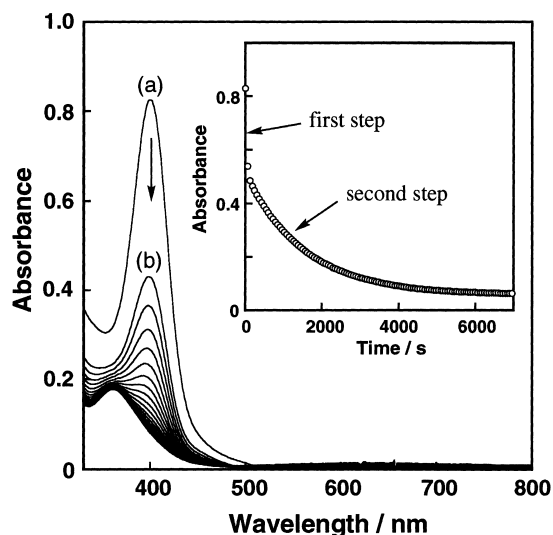
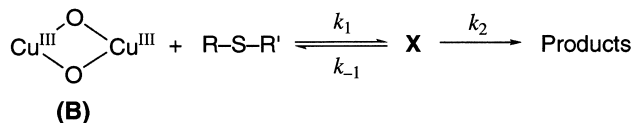


Fig. 11. Spectral change (300 s interval) observed upon addition of thioanisole ($1.0 \times 10^{-3}\text{ M}$) into an acetone solution of $[\text{Cu}^{\text{III}}_2(\text{H}^{\text{EtBz-d2}}\text{Py1})_2(\mu\text{-O})_2](\text{PF}_6)_2$ ($5 \times 10^{-5}\text{ M}$) at $-80\text{ }^{\circ}\text{C}$. Inset: Time course of the absorbance change at 400 nm.⁵⁸



Scheme 7.

tope labeling experiment using $^{18}\text{O}_2$ demonstrated that oxygen atom source of the product was indeed dioxygen.⁵⁸

The time course of the initial rapid process [(a) to (b) in Fig. 11] could be followed when the reaction was carried out at a lower temperature ($-94\text{ }^{\circ}\text{C}$).⁵⁸ The initial rapid process followed first-order kinetics, and plot of the pseudo-first-order

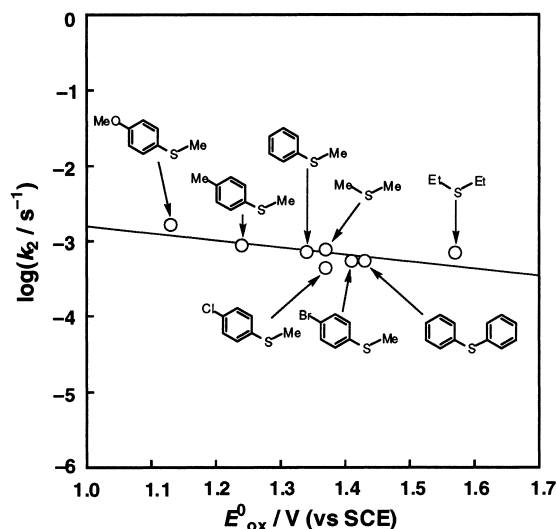


Fig. 12. Plot of $\log(k_2)$ against the oxidation potential (E^0_{ox}) of sulfides for the oxo-transfer reaction (the second process) in acetone at -80°C .⁵⁸

rate constant ($k_{\text{obs}(1)}$) against the substrate concentration provided a linear line with an intercept on the y-axis.⁵⁸ Existence of such an intercept on the y-axis indicates that the initial rapid decrease in absorbance at 400 nm is due to a process to reach an equilibrium between the bis(μ -oxo) complex (**B**) and an intermediate complex **X** (see Scheme 7). The slope of such a line corresponds to the rate constant for the forward reaction (k_1) and the intercept affords the rate constant of the backward reaction (k_{-1}). Then, the k_1/k_{-1} ratio corresponds to the formation constant (K) of the intermediate **X**. The equilibrium constant K can also be obtained from the absorbance change ($\Delta A = A_0 - A$) in the first rapid process, which increases with increasing substrate concentration to reach a constant value. Then, the K value for $\text{C}_6\text{H}_5\text{SMe}$ was also determined by fitting the titration data to the equation $\Delta A = \Delta A_{\infty} K[\text{Sulfide}]/(1 + K[\text{Sulfide}])$ as $(6.2 \pm 0.7) \times 10^3 \text{ M}^{-1}$. The result agreed within experimental errors with the value determined kinetically from the k_1/k_{-1} ratio, $(6.0 \pm 0.6) \times 10^3 \text{ M}^{-1}$.⁵⁸ Such an agreement strongly supports the formation of the intermediate complex **X**. Stack and co-workers have suggested that coordination of exogenous substrates such as alcohols to the metal center of the bis(μ -oxo)dicopper(III) core is a prerequisite for the *dehydrogenation* of the substrates.⁵⁹ Such an interaction between the sulfide and the bis(μ -oxo)dicopper(III) core also plays an essential role in the *oxo-transfer reaction* (Scheme 6), although the structural details of the intermediate **X** have yet to be elucidated.

The second slow process was then followed at the higher temperature (-80°C); results demonstrated that it was also a first-order reaction, but that the first-order rate constant ($k_{\text{obs}(2)}$) of this process was independent of the substrate concentration (i.e., $k_{\text{obs}(2)} = k_2$ in Scheme 7).⁵⁸ This clearly indicates that the second slow process is a unimolecular reaction of the intermediate **X** to the products. A plot of $\log k_2$ vs the oxidation potentials of several sulfide derivatives (E^0_{ox}) is shown in Fig. 12, where the slope of the straight line is significantly small (-0.94).

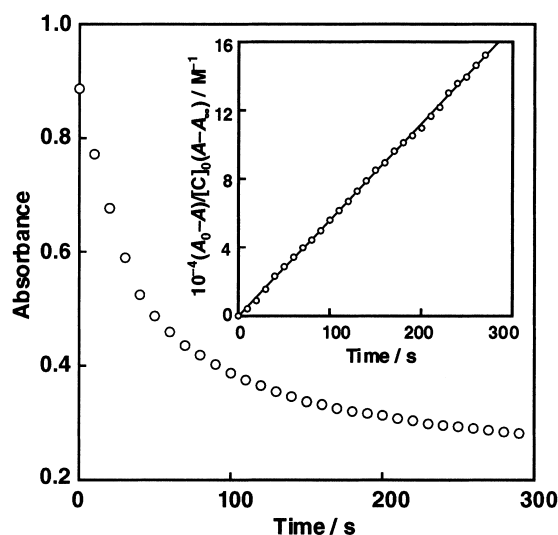


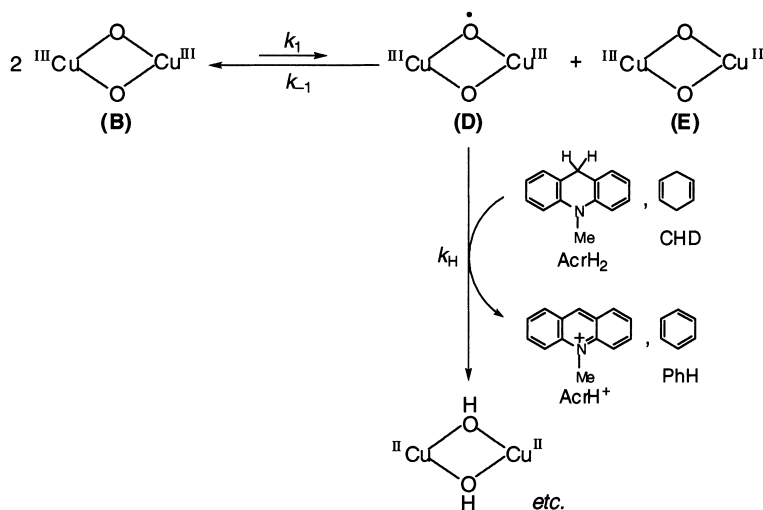
Fig. 13. Time course for the reaction of 10-methyl-9,10-dihydroacridine ($5.0 \times 10^{-4} \text{ M}$) and the bis(μ -oxo)dicopper(III) complex ($5.0 \times 10^{-5} \text{ M}$) in acetone at -94°C under Ar. Inset: Second-order plot based on the decrease of the absorbance at 400 nm.⁶²

Watanabe, Fukuzumi and co-workers have demonstrated that oxygenation of sulfides by compound **I** of horseradish peroxidase involves the electron transfer process as the key step; the slope of the same type of plot is quite negative (-10.5).⁶⁰ In contrast to this, the oxygenation of the same series of sulfides by $(\text{P}^{+\bullet})\text{Fe(IV)=O}$ ($\text{P}^{+\bullet}$: π -cation radical of porphyrin) in a model system proceeds via direct oxygen atom transfer, in which the slope becomes less negative (-2.3). This indicates that the rate of direct oxygen atom transfer is rather insensitive to the E^0_{ox} value, showing a sharp contrast with the oxygenation via electron transfer. Thus, the observed small slope in Fig. 12 also indicates that the oxygenation of sulfides by the bis(μ -oxo)dicopper(III) complex proceeds via a direct oxygen atom transfer mechanism rather than by one involving an electron transfer process.⁵⁸ Oxygen atom transfer from the bis(μ -oxo)dicopper(III) complex of $^{\text{H}}\text{Py1}^{\text{EtBz-d2}}$ to phosphines also proceeds to give the corresponding phosphine oxides.⁶¹

C–H Bond Activation of External Substrates with the Bis(μ -oxo)dicopper(III) Complex

We have so far overviewed the intermolecular oxygenation of phenolates to catechols by the $(\mu\text{-}\eta^2\text{:}\eta^2\text{-peroxo})\text{dicopper(II)}$ complex (**A**) and the intramolecular aliphatic hydroxylation and intermolecular oxygenation of sulfides to sulfoxides by the bis(μ -oxo)dicopper(III) complex (**B**). However, neither olefin epoxidation nor hydroxylation of externally added hydrocarbons occur with the peroxo and bis(μ -oxo) dicopper complexes.⁶¹ Nonetheless, examination of the intermolecular reaction between the bis(μ -oxo)dicopper(III) complex and an activated C–H bond such as in 10-methyl-9,10-dihydroacridine (AcrH_2) and 1,4-cyclohexadiene (CHD) has provided a new aspect in the chemistry of dinuclear copper dioxygen complexes (vide infra).⁶²

Treatment of AcrH_2 with the bis(μ -oxo)dicopper(III) complex supported by $^{\text{H}}\text{Py1}^{\text{EtBz-d2}}$ in acetone at -94°C under Ar



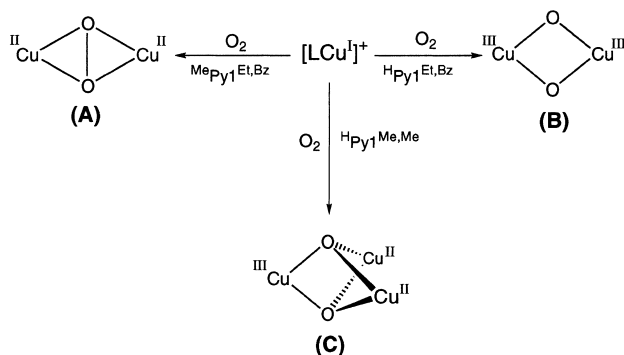
Scheme 8.

atmosphere resulted in quantitative formation of AcrH^+ (*N*-methylacridinium ion).⁶² Oxidation of CHD also proceeded smoothly to produce the corresponding oxidation products, i.e., benzene.⁶² To our surprise, the reaction was found to obey *second-order kinetics* even in the presence of a large excess substrate, as shown in Fig. 13.⁶² The second-order dependence on the bis(μ -oxo)dicopper(III) intermediate has also been confirmed by the result that the second-order rate constants k_{obs} obtained at various initial concentrations of the bis(μ -oxo) complex were inversely proportional to the initial concentration of bis(μ -oxo), as would be expected from the equation of the second-order plot: $(A_0 - A)/\{(A - A_\infty)[\text{bis}(\mu\text{-oxo})]_0\} = k_{\text{obs}}t$.⁶² The second-order rate constant k_{obs} was then plotted against the substrate concentration to demonstrate the first-order dependence of k_{obs} on [substrate], from which the third-order rate constant k_3 was determined as $1.2 \times 10^6 \text{ M}^{-2} \text{ s}^{-1}$ from the slope.⁶² The same kinetic behavior (the second-order dependence on bis(μ -oxo) and the first-order dependence on [substrate]) was observed in the reaction with CHD, and the k_3 value at -94°C was determined as $1.5 \times 10^4 \text{ M}^{-2} \text{ s}^{-1}$.⁶² In addition, a large primary kinetic deuterium isotope effect ($k_3^{\text{H}}/k_3^{\text{D}} = 22.7$) was obtained at -94°C when AcrD_2 (AcrD_2 = the 9,9-dideuterated analog of AcrH_2) was used in place of AcrH_2 .⁶² The $k_3^{\text{H}}/k_3^{\text{D}}$ value is significantly larger than the primary kinetic deuterium isotope effect (3.0) reported for the hydrogen abstraction from AcrH_2 by hydroperoxyl radical (HO_2^\bullet).⁶³ Such a large primary kinetic deuterium isotope effect indicates that a tunneling hydrogen transfer process is involved in the rate-determining step of the C–H bond activation with the bis(μ -oxo) complex. However, the direct reaction between bis(μ -oxo) complex and AcrH_2 would afford a first-order dependence of the rate with respect to the concentration of each reactant, contrary to the present experimental observation.

One of the possible explanations for such an unusual kinetic behavior {the *second-order* dependence on bis(μ -oxo)} is the following. Disproportionation of two molecules of the bis(μ -oxo)dicopper(III) complexes may afford one molecule of (μ -oxo)(μ -oxyl radical)dicopper(III) (**D**) and one molecule of

bis(μ -oxo)Cu(II)Cu(III) (**E**), the former of which is a real active species for the C–H bond activation (hydrogen atom abstraction) of the substrates (Scheme 8).⁶² In such a case, the reaction is second-order with respect to bis(μ -oxo), as experimentally observed. Unfortunately, however, we could not obtain any direct evidence for such an intermediate, since the equilibrium of the disproportionation reaction may lie far to the left, i.e., to the starting material [bis(μ -oxo)dicopper(III) complex (**B**)]. Alternatively two molecules of the bis(μ -oxo)dicopper(III) intermediate may function in unison (e.g., via a tetranuclear copper-oxo complex) to oxidize the substrate. At present, however, it is extremely difficult to distinguish between the disproportionation complex in Scheme 8 and a tetranuclear copper-oxo complex, since such a complex could not be detected because of the facile dissociation of the complex ($k_{-1} \gg k_1$ in Scheme 8).⁶²

The present reaction is the first example of the C–H bond activation of external non-coordinative substrates such as AcrH_2 and CHD with a bis(μ -oxo)dicopper(III) complex (**B**), where participation of a new copper-active oxygen species like a (μ -oxo)(μ -oxyl radical)dicopper(III) (**D**) or a tetranuclear copper-oxo complex is suggested by the kinetic data. As demonstrated previously, the aliphatic ligand hydroxylation proceeds intramolecularly in the bis(μ -oxo)dicopper(III) core. This is illustrated in Scheme 5, where the reaction proceeds via a stepwise mechanism involving hydrogen atom abstraction, followed by hydroxyl radical rebound or its concerted variant. The bond dissociation energies of AcrH_2 and CHD have been reported as ca. 72 and 75 kcal/mol, respectively, and that of the benzylic C–H bond is about 85 kcal/mol.⁶⁴ As demonstrated here, the intermolecular C–H bond activation of the external substrate such as AcrH_2 and CHD having the lower bond dissociation energy, requires a more reactive species such as (μ -oxo)(μ -oxyl radical)dicopper(III) (**D** in Scheme 8), while the intramolecular C–H bond activation of the ligand sidearm, which may have a higher bond dissociation energy, is accomplished in the less reactive bis(μ -oxo)dicopper(III) core (**B**). Thus, it is apparent that close contact between the substrate and the active oxo species is required for the efficient oxygen-



Scheme 9.

ation reactions. In the cases of oxygenation of phenolates by the $(\mu\text{-}\eta^2\text{:}\eta^2\text{-peroxo})$ dicopper(II) complex (A) and sulfoxidation by the bis(μ -oxo)dicopper(III) complex (B), such a close contact between the substrate and the active oxygen species is achieved by the coordination of the substrate to the metal center (vide ante). In the case of non-coordinative substrates such as AcrH₂ and CHD, however, such a close contact between the substrate and the metal-oxo species could not be attained. In such a case, a more reactive oxidant such as $(\mu\text{-oxo})(\mu\text{-oxyl radical})$ dicopper(III) complex (D) is required. In the enzymatic system, on the other hand, substrate binding into the active site pocket usually occurs to accomplish the close contact between the substrate and the catalytic center (so-called proximity effects).

Ligand Effects on Copper(I)-Dioxygen Reactivity in the Didentate Ligand System

As described earlier, a subtle change in the tridentate ligand system of $\text{R}^i\text{Py}2^{\text{R}}$ results in a drastic change in the structure and reactivity of the copper(I) complexes.^{22,25} Such effects induced by the subtle differences in the ligand structure have also been seen in the didentate ligand system ($\text{H}^i\text{Py}1^{\text{Et,Bz}}$ vs $\text{Me}^i\text{Py}1^{\text{Et,Bz}}$, vide infra).

Treatment of a copper(I) complex supported by a modified didentate ligand $\text{Me}^i\text{Py}1^{\text{Et,Bz}}$ ($\text{R} = \text{Me}$, $\text{R}_1 = \text{Et}$, $\text{R}_2 = -\text{CH}_2\text{Ph}$ in Chart 1) with dioxygen at -94°C in acetone gave an oxygenated intermediate exhibiting an absorption band at 365 nm ($\epsilon = 17,900 \text{ M}^{-1} \text{ cm}^{-1}$) together with a weak band at 518 nm ($860 \text{ M}^{-1} \text{ cm}^{-1}$).⁶⁵ The resonance Raman spectrum of the oxygenated solution provided Raman enhanced peaks at 737 and 284 cm^{-1} (with $^{16}\text{O}_2$), the former of which shifted to 696 cm^{-1} upon $^{18}\text{O}_2$ -substitution.⁶⁵ The Raman band around $280\text{--}290 \text{ cm}^{-1}$ has recently been assigned to an A_g "accordion" mode of the Cu_2O_2 peroxo core involving predominantly Cu–Cu motion.⁶⁶ The stoichiometry of the reaction was $\text{Cu}:\text{O}_2 = 2:1$ (± 0.05) and the solution was ESR silent.⁶⁵ These results unambiguously demonstrate that the Cu_2/O_2 intermediate has a $\mu\text{-}\eta^2\text{:}\eta^2\text{-peroxo}$ bridge.⁶⁷ This result is a sharp contrast to the fact that the ligand $\text{H}^i\text{Py}1^{\text{Et,Bz}}$ predominantly affords the bis(μ -oxo)dicopper(III) complex under otherwise the same experimental conditions (Scheme 9).^{58,62}

The $(\mu\text{-}\eta^2\text{:}\eta^2\text{-peroxo})$ dicopper(II) complex (A) and the bis(μ -oxo)dicopper(III) complex (B) are known to have similar thermodynamic stability such that changes in ligand substitu-

ents as well as solvent and/or counter anion are sufficient to result in formation of one or the other form.^{41,49,68} Steric repulsion between the bulky substituents of the capping ligands as well as the interaction between the Cu_2O_2 core and solvent and/or counter anion have been invoked as the major factors that control the equilibrium position between the two species, although the mechanistic details of their functions have yet to be clearly understood.^{41,49,68}

The selective formation of the $(\mu\text{-}\eta^2\text{:}\eta^2\text{-peroxo})$ dicopper(II) complex (A) using a didentate ligand ($\text{Me}^i\text{Py}1^{\text{Et,Bz}}$) can be easily explained by steric repulsion between the 6-methyl group and the metal center, which inhibits close approach of Cu to the nitrogen. The donor ability of the nitrogen is also reduced by the steric effect of the 6-methyl group.⁶⁹ In contrast, a short Cu–N_{py} distance ($\sim 1.9 \text{ \AA}$) required for formation of the high valent bis(μ -oxo)dicopper species (B) can be readily achieved using $\text{H}^i\text{Py}1^{\text{Et,Bz}}$ without the 6-methyl group.⁷⁰ Such steric and/or electronic effects of the 6-methyl group has also been found in the tridentate ligand system $\text{Me}^i\text{Py}2^{\text{Phe}}$ as described above.²⁵

The $(\mu\text{-}\eta^2\text{:}\eta^2\text{-peroxo})$ dicopper(II) complex (A) generated using the methylated didentate $\text{Me}^i\text{Py}1^{\text{Et,Bz}}$ decomposed gradually to afford the oxidative *N*-dealkylation products (benzaldehyde and *N*-ethyl-2-(2-pyridyl)-ethylamine). Eyring plots for the decomposition process with $\text{Me}^i\text{Py}1^{\text{Et,Bz}}$ and its didueterated ligand $\text{Me}^i\text{Py}1^{\text{Et,Bz-d2}}$ are very close to those obtained for the aliphatic ligand hydroxylation reaction in the $(\mu\text{-}\eta^2\text{:}\eta^2\text{-peroxo})$ dicopper(II) core supported by the tridentate ligand $\text{H}^i\text{Py}2^{\text{Phe}}$ (Fig. 9) in which O–O bond homolysis is rate-determining.²² The KIE value was relatively small (3.5 at -80°C) and the value was extrapolated to become unity at -16°C .⁶⁵ Furthermore, the activation parameters ($\Delta H^\ddagger = 7.5 \pm 0.1 \text{ kcal mol}^{-1}$, $\Delta S^\ddagger = -28.9 \pm 0.5 \text{ cal K}^{-1} \text{ mol}^{-1}$, $\Delta H^\ddagger = 9.8 \pm 0.6 \text{ kcal mol}^{-1}$, $\Delta S^\ddagger = -20.1 \pm 3.4 \text{ cal K}^{-1} \text{ mol}^{-1}$) were fairly close to those reported for the aliphatic ligand hydroxylation in the $(\mu\text{-}\eta^2\text{:}\eta^2\text{-peroxo})$ dicopper(II) complex supported by a tridentate ligand $\text{H}^i\text{Py}2^{\text{Phe}}$.²² Thus, in this case as well, the O–O bond homolysis of the peroxo species may be involved in the rate-determining step and the bis(μ -oxo)dicopper(III) species thus generated may be the actual active species for the oxidative *N*-dealkylation reaction as suggested for the aliphatic ligand hydroxylation reaction in the $\text{H}^i\text{Py}2^{\text{Phe}}$ system.

Decomposition of the bis(μ -oxo)dicopper(III) complex (B) supported by $\text{H}^i\text{Py}1^{\text{Et,Bz}}$ also led to the oxidative *N*-dealkylation reaction of the benzyl group.⁶⁵ In this case, however, a very large kinetic deuterium isotope effect (KIE) of 32.9 (at -55°C) was obtained. In addition, the activation parameters ($\Delta H^\ddagger = 13.1 \pm 0.2 \text{ kcal mol}^{-1}$, $\Delta S^\ddagger = -7.3 \pm 1.1 \text{ cal K}^{-1} \text{ mol}^{-1}$, $\Delta H^\ddagger = 15.9 \pm 0.6 \text{ kcal mol}^{-1}$, $\Delta S^\ddagger = -1.3 \pm 2.7 \text{ cal K}^{-1} \text{ mol}^{-1}$)⁶⁵ are similar to those reported for the aliphatic ligand hydroxylation in the bis(μ -oxo)dicopper(III) core supported by $\text{H}^i\text{Py}1^{\text{Et,Phe}}$.⁵⁰ These results clearly indicate that the oxidative *N*-dealkylation reaction proceeds via a similar mechanism: hydrogen atom abstraction and oxygen rebound or its concerted variant (cf. Scheme 5).

Another interesting result was obtained with a didentate ligand carrying the smallest *N*-alkyl substituents $\text{H}^i\text{Py}1^{\text{Me,Me}}$ ($\text{R}^1 = \text{R}^2 = \text{Me}$ in Chart 1).⁶⁵ Treatment of a 5.0 mM acetone solution of $[\text{Cu}^{\text{I}}(\text{H}^i\text{Py}1^{\text{Me,Me}})(\text{CF}_3\text{SO}_3)]$ with dioxygen at -94°C resulted in color change of the solution from pale yellow to

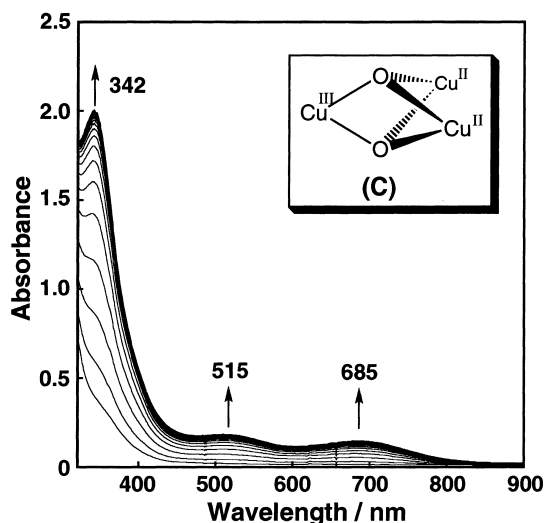


Fig. 14. Spectral change observed upon introduction of O_2 gas into an acetone solution of $[Cu^I(HPy1^{MeMe})(CF_3SO_3)]$ (5.0×10^{-3} M) at $-94^\circ C$.

dark brown. A typical example of the spectral change for the oxygenation reaction of copper(I) complex is shown in Fig. 14 (measured by using a 1 mm path length UV cell), where a strong absorption band at 342 nm ($\epsilon = 12,000 \text{ M}^{-1} \text{ cm}^{-1}$) rapidly appears together with two small bands at 515 ($1,000$) and 685 nm ($800 \text{ M}^{-1} \text{ cm}^{-1}$).⁶⁵ The final spectrum of the reaction is significantly different from that of the bis(μ -oxo)dicopper(III) complex generated in the reaction of $[Cu^I(HPy1^{Et,Bz})(CH_3CN)]PF_6$ with O_2 in acetone,^{58,62} but is fairly close to that of the bis(μ_3 -oxo)tricopper(II,II,III) complex (C in Scheme 9) reported by Stack et al [$\lambda_{\text{max}} = 355$ ($15,000$), 480 ($1,400$) and 620 nm ($800 \text{ M}^{-1} \text{ cm}^{-1}$)].⁷¹ Stoichiometry of $Cu:O_2$ in this reaction was determined by manometry as 3:1 (± 0.1). The acetone solution of the oxygenated intermediate was ESR silent. These features of the oxygenated intermediate are quite similar to those of the reported trinuclear mixed valence copper(II,II,III) bis(μ_3 -oxo) complex (C). This strongly indicates formation of the same type of intermediate in the present $HPy1^{MeMe}$ system. Mechanistic studies on the formation process have suggested that a bis(μ -oxo)dicopper(III) complex is involved as the precursor of the bis(μ_3 -oxo) trinuclear copper(II,II,III) product.⁶⁵

Four-electron reduction of dioxygen to water is accomplished at a trinuclear copper active center in multi-copper enzymes such as ascorbate oxidase, laccase and ceruloplasmin.¹² A trinuclear copper site has also been invoked as the reaction center of particulate methane monooxygenase (pMMO), which catalyzes hydroxylation of methane to methanol.⁷² In spite of such important roles of the trinuclear copper active sites in biological dioxygen processing, only a limited number of model compounds of trinuclear copper/dioxygen complexes have been reported so far.^{71,73} The present reaction models the four-electron reduction of dioxygen at the trinuclear copper active site in the enzymes, providing another possible reaction pattern in copper(I)-dioxygen chemistry in model systems.

Concluding Remarks

By using a series of simple tridentate and didentate 2-(2-pyridyl)ethylamine ligands, we have successfully generated (μ - η^2 : η^2 -peroxo)dicopper(II) (A), bis(μ -oxo)dicopper(III) (B), and bis(μ_3 -oxo)tricopper(II,II,III) (C) complexes at low temperature. The tridentate ligands $HPy2^R$ predominantly provide the (μ - η^2 : η^2 -peroxo)dicopper(II) complex, with which we have developed an efficient model reaction of tyrosinase, that is intermolecular oxygenation of phenolates to the corresponding catechols.²¹ In this reaction, electrophilic aromatic substitution mechanism by the peroxo species has been proposed, based on the results of product analysis and kinetics.²¹ The tridentate ligand with *N*-phenethyl substituent $HPy2^{Phe}$ provided another interesting reactivity in copper(I)/dioxygen chemistry, that is intramolecular aliphatic ligand hydroxylation.⁴⁶ Detailed kinetic analysis on this reaction has suggested that the (μ - η^2 : η^2 -peroxo)dicopper(II) complex is not a real active oxygen intermediate but that O–O bond cleavage does occur prior to the C–H bond activation.²² Ligand modification by removing one of the pyridine nuclei of the tridentate ligand to make the didentate ligand allowed direct detection of the real active oxygen intermediate, bis(μ -oxo)dicopper(III) complex, in the aliphatic ligand hydroxylation.⁵⁰

Replacement of the phenethyl group by deuterated benzyl group in the didentate ligand led to stabilization of the bis(μ -oxo)dicopper(III) complex, allowing us to investigate the reactivity of the bis(μ -oxo)dicopper(III) complex toward external substrates. Oxygenation of sulfides to the corresponding sulfoxide by the bis(μ -oxo)dicopper(III) complex is shown to proceed through formation of a binary complex between the substrate and metal-oxo species.⁵⁸ A direct oxygen atom transfer mechanism rather than an electron-transfer mechanism has been suggested by the observed small dependence of the reaction rate on the oxidation potential of the substrates.⁵⁸ The kinetic studies on the reaction between the bis(μ -oxo)dicopper(III) complex and 10-methyl-9,10-dihydroacridine (AcH_2) and 1,4-cyclohexadiene (CHD) have suggested formation of a new active oxygen intermediate such as (μ -oxo)(μ -oxyl radical)dicopper(III) complexes (D) or a tetranuclear copper-oxygen species.⁶²

Further modification of the tridentate and didentate ligands have expanded the scope of copper(I) dioxygen chemistry. Introduction of a methyl group either at the benzylic position of the *N*-phenethyl substituent or at the 6-position of the pyridine nucleus of the tridentate ligands resulted in a loss of reactivity of their copper(I) complexes toward molecular oxygen.²⁵ Crystal structures of the copper(I) complexes suggested that the existence of a d– π interaction between the copper(I) ion and the phenyl group of the ligand sidearm and the stronger binding of acetonitrile to the metal center induced by the methyl group are the major factors for such a drastic change in the reactivity of the copper(I) complexes.²⁵ Introduction of the 6-methyl group into the didentate ligand also led to a drastic change in the structure of the oxygenated products of the copper(I) complexes.⁶⁵ Namely, $MePy1^{Et,Bz}$ predominantly afforded a (μ - η^2 : η^2 -peroxo)dicopper(II) complex, while $HPy1^{Et,Bz}$ gave a bis(μ -oxo)dicopper(III) complex under the same experimental conditions.⁶⁵ Such a steric effect and an electronic ef-

fect by the 6-methyl group have also been found in dicopper(I) complexes including a disulfide bond in the supporting ligands.⁷⁴ On the other hand, the didentate ligand with the smallest *N*-substituent (^HPy1^{Me,Me}) made it possible to generate a mixed valence bis(μ -oxo) trinuclear copper(II,II,III) complex at a relatively high concentration (~5 mM).⁶⁵ Reduction of the steric bulkiness may allowed the bis(μ -oxo)dicopper(III) complex to react with another copper(I) starting material, generating the trinuclear complex.

In addition to the ligand effects on the copper(I) dioxygen reactivity, we have also investigated metal ion effects on the dioxygen activation mechanism using nickel complex with the *tridentate ligands*. Bis(μ -oxo)dinickel(III) complexes exhibiting similar spectroscopic features to those of the bis(μ -oxo)dicopper(III) complexes were always formed in the reaction of the bis(μ -hydroxo)dinickel(II) or bis(μ -methoxo)dinickel(II) complexes with H₂O₂, regardless the type of tridentate ligand used (^HPy2^R, Nn and XYL, see Charts 1–4).^{75,76} Thus, it is apparent that the higher oxidation state is more easily assessed in the nickel case to enhance the O–O bond homolysis of the peroxo species. The bis(μ -oxo)dinickel(III) species exhibits a similar reactivity to that of the bis(μ -oxo)dicopper(III) complexes but has no ability to promote the aromatic hydroxylation reaction. This result is also consistent with our proposed mechanism of the phenolate oxygenation by the (μ - η^2 : η^2 -peroxo)dicopper(II) complex, where O–O bond homolysis does not occur prior to the C–O bond formation (Scheme 2). Although further study remains to disclose the mechanistic details for the ligand control of the copper(I)-dioxygen reactivity, we hope the results presented in this account will help the understanding and the application of the dioxygen activation mechanism by the non-heme transition metal complexes.

A large part of the work presented in this account has been done by Masayasu Taki of Osaka University as his doctoral research during 1998–2001. The authors thank the collaborations with Professor Teizo Kitagawa and Mr. Shigenori Nagatomo of Institute for Molecular Science, Okazaki, Professor William B. Tolman and Professor Laurence Que, Jr. of the University of Minnesota, Professor Kenneth D. Karlin of Johns Hopkins University and all other people indicated in the list of our papers. These works were financially supported in part by Grants-in-Aid for Scientific Research Priority Area (Nos. 11228205, 11228206) and Grants-in-Aid for Scientific Research (Nos. 11440197, 12874082 and 13480189) from the Ministry of Education, Culture, Sports, Science and Technology.

References

- 1 "Active Oxygen in Biochemistry," ed by J. S. Valentine, C. S. Foote, A. Greenberg, and J. F. Liebman, Chapman and Hall, London (1995).
- 2 "Active Oxygen in Chemistry," ed by C. S. Foote, J. S. Valentine, A. Greenberg, and J. F. Liebman, Chapman and Hall, London (1995).
- 3 "Oxygenases and Model Systems," ed by T. Funabiki, Kluwer Academic Publishers, Dordrecht (1997).
- 4 "Biomimetic Oxidations Catalyzed by Transition Metal Complexes," ed by B. Meunier, Imperial College Press, London

(1999).

- 5 "Metal-Oxo and Metal-Peroxo Species in Catalytic Oxidations," ed by B. Meunier, Springer, Berlin (2000).
- 6 S. E. V. Phillips, *J. Mol. Biol.*, **142**, 531 (1980).
- 7 "Cytochrome P-450. Structure, Mechanism, and Biochemistry," ed by P. R. Ortiz de Montellano, Plenum Press, New York (1986).
- 8 "Handbook of Metalloproteins, Volume 1 & 2," ed by A. Messerschmidt, R. Huber, T. Poulos, and K. Wieghardt, John Wiley & Sons, Chichester (2001).
- 9 "Handbook on Metalloproteins," ed by I. Bertini, A. Sigel, and H. Sigel, Marcel Dekker, New York (2001).
- 10 K. D. Karlin, P. L. Dahlstrom, L. T. Dipierro, R. A. Simon, and J. Zubieta, *J. Coord. Chem.*, **11**, 61 (1980).
- 11 M.-A. Kopf and K. D. Karlin, "Biomimetic Oxidations Catalyzed by Transition Metal Complexes," ed by B. Meunier, Imperial College Press, London (1999), pp. 309–362.
- 12 E. I. Solomon, U. M. Sundaram, and T. E. Machonkin, *Chem. Rev.*, **96**, 2563 (1996).
- 13 A. Volbeda and W. G. J. Hol, *J. Mol. Biol.*, **209**, 249 (1989).
- 14 In the case of *L. polyphemus* hemocyanin, however, the intercopper distance is reported as 4.6 Å. It was suggested that these two active site conformations represent "relaxed" (high oxygen affinity) and "tense" (low oxygen affinity) states of the proteins; B. Hazes, K. A. Magnus, C. Bonaventura, J. Bonaventura, K. H. Kalk, and W. G. J. Hol, *Protein Sci.*, **2**, 597 (1993).
- 15 K. A. Magnus, B. Hazes, H. Ton-That, C. Bonaventura, J. Bonaventura, and W. G. J. Hol, *Protein*, **19**, 302 (1994).
- 16 E. I. Solomon, B. L. Hemming, and D. E. Root, "Bioinorganic Chemistry of Copper," ed by K. D. Karlin and Z. Tyeklar, Chapman & Hall, New York (1993), pp. 3–20.
- 17 N. Kitajima, K. Fujisawa, and Y. Moro-oka, *J. Am. Chem. Soc.*, **111**, 8975 (1989).
- 18 K. D. Karlin, Y. Gultneh, J. P. Hutchinson, and J. Zubieta, *J. Am. Chem. Soc.*, **104**, 5240 (1982); K. D. Karlin, M. S. Haka, R. W. Cruse, and Y. Gultneh, *J. Am. Chem. Soc.*, **107**, 5828 (1985).
- 19 M. Kodera, K. Katayama, Y. Tachi, K. Kano, S. Hirota, S. Fujinami, and M. Suzuki, *J. Am. Chem. Soc.*, **121**, 11006 (1999).
- 20 I. Sanyal, M. Mahroof-Tahir, M. S. Nasir, P. Ghosh, B. I. Cohen, Y. Gultneh, R. W. Cruse, A. Farooq, K. D. Karlin, S. Liu, and J. Zubieta, *Inorg. Chem.*, **31**, 4322 (1992).
- 21 S. Itoh, H. Kumei, M. Taki, S. Nagatomo, T. Kitagawa, and S. Fukuzumi, *J. Am. Chem. Soc.*, **123**, 6708 (2001).
- 22 S. Itoh, H. Nakao, L. M. Berreau, T. Kondo, M. Komatsu, and S. Fukuzumi, *J. Am. Chem. Soc.*, **120**, 2890 (1998).
- 23 E. Pidcock, S. DeBeer, H. V. Obias, B. Hedman, K. O. Hodgson, K. D. Karlin, and E. I. Solomon, *J. Am. Chem. Soc.*, **121**, 1870 (1999).
- 24 In the case of ^HPy2^{Me}, coexistence of a few percent of bis(μ -oxo)dicopper(III) complex has been demonstrated by X-ray crystallographic analysis, resonance Raman and EXAFS.²³
- 25 T. Osako, Y. Tachi, M. Taki, S. Fukuzumi, and S. Itoh, *Inorg. Chem.*, **40**, 6604 (2001).
- 26 W. S. Striejewske and R. R. Conry, *Chem. Commun.*, **1998**, 555.
- 27 Y. Shimazaki, H. Yokoyama, and O. Yamauchi, *Angew. Chem., Int. Ed.*, **38**, 2401 (1999).
- 28 T. Osako, Y. Tachi, and S. Itoh, unpublished results.
- 29 K. A. Magnus, H. Ton-That, and J. E. Carpenter, *Chem. Rev.*, **94**, 727 (1994).
- 30 K. D. Karlin, P. L. Dahlstrom, S. N. Cozzette, P. M.

- Scensny, and J. Zubieta, *J. Chem. Soc., Chem. Commun.*, **1981**, 881.
- 31 K. D. Karlin, J. C. Hayes, Y. Gultneh, R. W. Cruse, J. W. McKown, J. P. Hutchinson, and J. Zubieta, *J. Am. Chem. Soc.*, **106**, 2121 (1984).
- 32 M. S. Nasir, B. I. Cohen, and K. D. Karlin, *J. Am. Chem. Soc.*, **114**, 2482 (1992).
- 33 K. D. Karlin, M. S. Nasir, B. I. Cohen, R. W. Cruse, S. Kaderli, and A. D. Zuberbühler, *J. Am. Chem. Soc.*, **116**, 1324 (1994).
- 34 E. Pidcock, H. V. Obias, C. X. Zhang, K. D. Karlin, and E. I. Solomon, *J. Am. Chem. Soc.*, **120**, 7841 (1998).
- 35 N. Kitajima and Y. Moro-oka, *Chem. Rev.*, **94**, 737 (1994), and references cited therein.
- 36 S. Mahapatra, S. Kaderli, A. Llobet, Y.-M. Neuhold, T. Palanché, J. A. Halfen, V. G. Young, Jr., T. A. Kaden, L. Que, Jr., A. D. Zuberbühler, and W. B. Tolman, *Inorg. Chem.*, **36**, 6343 (1997), and references cited therein.
- 37 N. Kitajima, T. Koda, Y. Iwata, and Y. Moro-oka, *J. Am. Chem. Soc.*, **112**, 8833 (1990).
- 38 P. P. Paul, Z. Tyeklár, R. R. Jacobson, and K. D. Karlin, *J. Am. Chem. Soc.*, **113**, 5322 (1991).
- 39 H. V. Obias, Y. Lin, N. N. Murthy, E. Pidcock, E. I. Solomon, M. Ralle, N. J. Blackburn, Y.-M. Neuhold, A. D. Zuberbühler, and K. D. Karlin, *J. Am. Chem. Soc.*, **120**, 12960 (1998).
- 40 J. A. Halfen, V. G. Young, Jr., and W. B. Tolman, *Inorg. Chem.*, **37**, 2102 (1998).
- 41 V. Mahadevan, M. J. Henson, E. I. Solomon, and T. D. P. Stack, *J. Am. Chem. Soc.*, **122**, 10249 (2000).
- 42 Casella and coworkers have recently reported that their (μ - η^2 : η^2 -peroxo)dycopper(II) complex can react with an exogenous phenolate to yield the corresponding catechol. However, the low yield of the product (20% based on the dycopper complex) has precluded the kinetic and mechanistic investigation on the reaction between the peroxo intermediate and the phenolate; L. Santagostini, M. Gullotti, E. Monzani, L. Casella, R. Dillinger, and F. Tuczek, *Chem. Eur. J.*, **6**, 519 (2000).
- 43 The C–C coupling dimer became the major product when the phenol itself was used instead of the phenolate as in the case of other peroxo systems. In such a case, hydrogen atom abstraction from the phenol occurs to produce the corresponding phenoxyl radical leading to the C–C coupling reaction.
- 44 H. Decker, R. Dillinger, and F. Tuczek, *Angew. Chem., Int. Ed.*, **39**, 1591 (2000).
- 45 L. M. Sayre and D. V. Nadkarni, *J. Am. Chem. Soc.*, **116**, 3157 (1994); S. Mandal, D. Macikenas, J. D. Protasiewicz, and L. M. Sayre, *J. Org. Chem.*, **65**, 4804 (2000).
- 46 S. Itoh, T. Kondo, M. Komatsu, Y. Ohshiro, C. Li, N. Kanehisa, Y. Kai, and S. Fukuzumi, *J. Am. Chem. Soc.*, **117**, 4714 (1995).
- 47 S. Mahapatra, J. A. Halfen, and W. B. Tolman, *J. Am. Chem. Soc.*, **118**, 11575 (1996).
- 48 C. Kim, Y. Dong, and L. Que, Jr., *J. Am. Chem. Soc.*, **119**, 3635 (1997).
- 49 J. A. Halfen, S. Mahapatra, E. C. Wilkinson, S. Kaderli, V. G. Young Jr., L. Que Jr., A. D. Zuberbühler, and W. B. Tolman, *Science*, **271**, 1397 (1996).
- 50 S. Itoh, M. Taki, H. Nakao, P. L. Holland, W. B. Tolman, L. Que, Jr., and S. Fukuzumi, *Angew. Chem., Int. Ed.*, **39**, 398 (2000).
- 51 S. Mahapatra, J. A. Halfen, E. C. Wilkinson, G. Pan, X. Wang, V. G. Young, Jr., C. J. Cramer, L. Que, Jr., and W. B. Tolman, *J. Am. Chem. Soc.*, **118**, 11555 (1996).
- 52 S. Mahapatra, V. G. Young Jr., S. Kaderli, A. D. Zuberbühler, and W. B. Tolman, *Angew. Chem., Int. Ed. Engl.*, **36**, 130 (1997).
- 53 V. Mahadevan, Z. Hou, A. P. Cole, D. E. Root, T. K. Lal, E. I. Solomon, and T. D. P. Stack, *J. Am. Chem. Soc.*, **119**, 11996 (1997).
- 54 P. L. Holland, C. J. Cramer, E. C. Wilkinson, S. Mahapatra, K. R. Rodgers, S. Itoh, M. Taki, S. Fukuzumi, L. Que, Jr., and W. B. Tolman, *J. Am. Chem. Soc.*, **122**, 792 (2000).
- 55 M. J. Henson, P. Mukherjee, D. E. Root, T. D. P. Stack, and E. I. Solomon, *J. Am. Chem. Soc.*, **121**, 10332 (1999).
- 56 C. X. Zhang, H.-C. Liang, E. Kim, Q.-F. Gan, Z. Tyeklár, K.-C. Lam, A. L. Rheingold, S. Kaderli, A. D. Zuberbühler, and K. D. Karlin, *Chem. Commun.*, **2001**, 631.
- 57 P. L. Holland, K. R. Rodgers, and W. B. Tolman, *Angew. Chem., Int. Ed.*, **38**, 1139 (1999).
- 58 M. Taki, S. Itoh, and S. Fukuzumi, *J. Am. Chem. Soc.*, **124**, 998 (2002).
- 59 V. Mahadevan, J. L. DuBois, B. Hedman, K. O. Hodgson, T. D. P. Stack, *J. Am. Chem. Soc.*, **121**, 5583 (1999).
- 60 Y. Goto, T. Matsui, S. Ozaki, Y. Watanabe, and S. Fukuzumi, *J. Am. Chem. Soc.*, **121**, 9497 (1991).
- 61 M. Taki, S. Fukuzumi, and S. Itoh, unpublished results.
- 62 M. Taki, S. Itoh, and S. Fukuzumi, *J. Am. Chem. Soc.*, **123**, 6203 (2001).
- 63 S. Fukuzumi, M. Ishikawa, and T. Tanaka, *J. Chem. Soc., Perkin Trans. 2*, **1989**, 1037.
- 64 M. Anne, S. Fraoua, V. Grass, J. Moiroux, and J.-M. Savéant, *J. Am. Chem. Soc.*, **120**, 2951 (1998); C. R. Goldsmith, R. T. Jonas, and T. D. P. Stack, *J. Am. Chem. Soc.*, **124**, 83 (2002), and references cited therein.
- 65 M. Taki, S. Teramae, S. Nagatomo, Y. Tachi, T. Kitagawa, S. Itoh, and S. Fukuzumi, *J. Am. Chem. Soc.*, **124**, 6367 (2002).
- 66 M. J. Henson, V. Mahadevan, T. D. P. Stack, and E. I. Solomon, *Inorg. Chem.*, **40**, 5068 (2001).
- 67 This is the first example of quantitative formation of the (μ - η^2 : η^2 -peroxo)dycopper(II) complex (**A**) using a *didentate* ligand.
- 68 W. B. Tolman, *Acc. Chem. Res.*, **30**, 227 (1997).
- 69 H. Nagao, N. Komeda, M. Mukaida, M. Suzuki, and K. Tanaka, *Inorg. Chem.*, **35**, 6809 (1996).
- 70 Interaction between two 6-methylpyridines and the copper(III) ion in the Suzuki's bis(μ -oxo)dycopper(III) complex supported by bis(6-methyl-2-pyridinylmethyl)(2-pyridinylmethyl)amine (Me₂TPA) is known to be very weak (Cu–N_{MePy}: 2.48, 2.55 Å) while the remaining pyridine without the substituent strongly bound to the metal center (Cu–N_{Py}: 1.91 Å) to stabilize the copper(III) state. See: H. Hayashi, S. Fujinami, S. Nagatomo, S. Ogo, M. Suzuki, A. Uehara, Y. Watanabe, and T. Kitagawa, *J. Am. Chem. Soc.*, **122**, 2124 (2000).
- 71 A. P. Cole, D. E. Root, P. Mukherjee, E. I. Solomon, and T. D. P. Stack, *Science*, **273**, 1848 (1996).
- 72 S. I. Chan, H. T. Nguyen, A. K. Shiemke, and M. E. Lidstrom, "Bioinorganic Chemistry of Copper," ed by K. D. Karlin and Z. Tyeklár, Chapman & Hall, New York (1993), pp. 184–195.
- 73 K. D. Karlin, Q.-F. Gan, A. Farooq, S. Liu, J. Zubieta, *Inorg. Chem.*, **29**, 2549 (1990).
- 74 S. Itoh, M. Nakagawa, and S. Fukuzumi, *J. Am. Chem. Soc.*, **123**, 4087 (2001).
- 75 S. Itoh, H. Bandoh, S. Nagatomo, T. Kitagawa, and S. Fukuzumi, *J. Am. Chem. Soc.*, **121**, 8945 (1999).
- 76 S. Itoh, H. Bandoh, M. Nakagawa, S. Nagatomo, T.

Kitagawa, K. D. Karlin, and S. Fukuzumi, *J. Am. Chem. Soc.*, **123**, 11168 (2001).



Shinobu Itoh was born in Fukui prefecture in 1958. He received his Doctor's degree in engineering under the supervision of Professor Toshio Agawa and Professor Yoshiki Ohshiro from Osaka University in 1986. Then, he joined Professor Ohshiro's group at Osaka University as Assistant Professor, where he worked on the chemistry of coenzyme PQQ and cofactor TTQ as well as model compounds of galactose oxidase. During that period, he spent a year (1987–1988) as a postdoctoral fellow in Professor Teddy G. Traylor's group at the University of California, San Diego, where he learned the chemistry of heme proteins. In 1994, he was promoted to Associate Professor and worked with Professor Shunichi Fukuzumi at Osaka University, when he started copper/dioxygen chemistry. In 1999, he moved to Osaka City University as a full Professor. His current research interest is focused on chemical modeling and application of novel active sites in biological systems.



Shunichi Fukuzumi was born in Nagoya in 1950. He received his Ph.D. degree under the supervision of Profs. T. Keii and Y. Ono from Tokyo Institute of Technology in 1978. He did postdoctoral work with Professor Jay K. Kochi at Indiana University from 1978 to 1981. After that, he joined the Department of Applied Chemistry of Osaka University and became a professor in 1994. His research interest is centered on mechanisms and catalysis in electron transfer chemistry of various organic compounds (in particular coenzyme analogs), organo-metallic compounds, and metal complexes.